A hybrid Hartree–Fock density functional theory study of $Li_xNi_{1-x}O$

2004 J. Phys.: Condens. Matter 16 S2811

(http://iopscience.iop.org/0953-8984/16/27/015)

INSTITUTE OF PHYSICS PUBLISHING JOURNAL OF PHYSICS: CONDENSED MATTER

J. Phys.: Condens. Matter **16** (2004) S2811–S2825 PII: S0953-8984(04)73695-4

A hybrid Hartree–Fock density functional theory study of $Li_xNi_{1-x}O$

W C Mackrodt[1] **and D S Middlemiss**

School of Chemistry, University of St Andrews, St Andrews, Fife KY16 9ST, UK

E-mail: wcm@st-and.ac.uk

Received 17 December 2003
Published 25 June 2004
Online at stacks.iop.org/JPhysCM/16/S2811
doi:10.1088/0953-8984/16/27/015

Abstract

Hybrid spin unrestricted Hartree–Fock density functional theory (UHF-DFT) calculations of $Li_xNi_{1-x}O$ indicate that within the range of exact exchange for which the electronic structures of the associated point defects, Li'_{Ni}, $h^\bullet$ and $(Li'_{Ni}–h^\bullet)^x$ are insulating, Li'_{Ni} is a largely inert defect with negligible effect on the electronic, magnetic and excitonic properties of the NiO host lattice. Over this range of exact exchange the free hole, $h^\bullet$, is essentially $d^8\underline{L}$ in nature, or O^- in chemical terms, with strong spatial and spin polaronic character. The differences in the electronic properties of the free, $h^\bullet$, and bound, $(Li'_{Ni}–h^\bullet)^x$, hole, notably the $d^8\underline{L}$–d^9 gap, are minimal so that their separate identification would seem to be unlikely.

1. Introduction

Despite decades of intense investigation, nickel oxide (NiO) continues to attract interest as a paradigm magnetic insulator [1]. In its ground state it is largely ionic, with an energy gap of ∼4 eV [2], leading to a widely held view that it is essentially a d^8 system, with local moments close to the Hund's rule value in the AF_2 alignment. On the other hand, the nature of the gap, and from this the first ionized, or hole state, has remained a matter of some debate. For many years the received view, based on simple descriptions of ionicity and valence, was that NiO is a Mott–Hubbard system and the first ionized state is close to d^7 (∼Ni^{3+}). Early first principles calculations based on density functional theory (DFT), mostly within the local density approximation [3], supported this view, albeit with unacceptably small energy gaps. However, in 1985, not long after an augmented plane wave (APW) DFT study by Terakura *et al* [3] found AF_2 MnO and NiO to be Mott–Hubbard insulators, Zaanen *et al* [4] proposed theoretical phase diagrams of the first row transition metal (TM) chalcoginides, based essentially on the Hubbard U and charge transfer, Δ, energies. These

[1] Author to whom any correspondence should be addressed.

diagrams classified the later TM oxides, including NiO, as charge-transfer systems with holes largely of O(2p) character, in contrast to the earlier oxides, notably TiO and VO, which, it was argued, possessed gap states of essentially d character, leading to $\sim d^{n-1}$ holes. Experimental support for $d^n\underline{L}$ holes in NiO was found in the O k-edge spectra of Li-doped NiO ($Li_xNi_{1-x}O$) in the range $0 \leqslant x \leqslant 0.5$, which showed the presence of empty O(p) states $\sim$4 eV below the conduction band edge [5]. Importantly, these data also confirmed the insulating nature of the first ionized state within the specified range of stoichiometry. Subsequent spectroscopic studies have confirmed these observations, notably in respect of the lower energy of the $d^n\underline{L}$ state in $Li_xNi_{1-x}O$ relative to d^7 [6–8].

By and large, more recent first principles calculations of NiO have concluded that the ground electronic state is essentially charge-transfer insulating. Spin unrestricted, periodic Hartree–Fock (UHF) calculations based on localized orbitals found NiO to be a largely ionic, charge-transfer magnetic insulator in the FM (ferromagnetic), AF_1 and AF_2 spin alignments with local moments close to the measured values, but, as expected, with an energy gap greatly in excess of the observed absorption edge [2]. DFT calculations within the SIC (self interaction correction) [10] and LDA + U (local density approximation plus additional local potential, U) [11] schemes have also attested to the charge transfer character of NiO, as have recent self-consistent GW calculations, which describe essentially the same physics as the UHF approach [12].

While the calculated ground state electronic structure clearly provides important clues as to the nature of the ionized state, such renormalization of the valence states that might accompany the removal of an electron cannot be accounted for in a quantitative way from the ground state. The most straightforward approach which allows such changes to be included self-consistently is to calculate the electronic structure of the ionized state directly; that is to say, by direct variational minimization of the total energy. Such calculations have been reported both for the bound hole in $Li_xNi_{1-x}O$ ($x = 0.25$ and 0.125) [13] and the free hole in NiO [14], but only at the UHF level of approximation. While these calculations have confirmed that both bound and free holes are essentially of $d^8\underline{L}$ character and that the overall states are insulating, UHF calculations neglect important aspects of electron correlation, which may have a significant effect on details of the hole state. These include the localization energy, the differences between the (hole) charge and spin densities, the local magnetism and the elementary excitations of the anion hole. To gauge how these and other aspects of hole states might vary with the explicit, self-consistent inclusion of electron correlation, and as part of a wider study, we have examined the so-called 'hybrid' approach to the single-particle description of the electronic structures of the Li-bound and free hole in NiO. Accordingly, this paper reports some of the results of this study, and it is a pleasure to dedicate it to the memory of Michael Norgett, with whom one of the authors (and others in this volume) examined some of the properties of holes in the later TMOs, more than 25 years ago [15].

2. Theoretical considerations

2.1. Defect states of $Li_xNi_{1-x}O$

At ambient temperature and pressure, solid solutions of the type $Li_xNi_{1-x}O$ are formed by the defect reactions

$$Li_2O(s) + 2Ni_{Ni}^{x} + \tfrac{1}{2}O_2(g) \rightarrow 2Li'_{Ni} + 2h^{\bullet} + 2NiO$$
$$Li'_{Ni} + h^{\bullet} \rightarrow (Li'_{Ni} - h^{\bullet})^{x}$$

in Kröger–Vink notation [16], where Li'_{Ni} corresponds to an isolated Li substituent at a Ni site, $h^{\bullet}$ to a free hole and $(Li'_{Ni}–h^{\bullet})^{x}$ to a bound hole nearest neighbour (nn) to Li'_{Ni}. In this notation

the superscripts $'$, $\bullet$, and x correspond to site charges of -1, $+1$ and 0 respectively, relative to the non-defective lattice. For present purposes we neglect higher aggregates such as dipolar complexes formed from $(Li'_{Ni}–h^{\bullet})^x$, so that our defect model for $Li_xNi_{1-x}O$ is that it consists of an NiO host lattice containing varying concentrations of Li'_{Ni}, $h^{\bullet}$ and $(Li'_{Ni}–h^{\bullet})^x$ defects, the associated electronic structures of which are the subject of this study. Lattice relaxation has been neglected throughout, largely because previous calculations [13, 14] have suggested that the associated energies are a few tenths of an electronvolt, which is small compared to the energies we are concerned with here, while changes to the charge and spin distributions were found to be negligible.

2.2. Hybrid Hamiltonians

While a fully many-body solution to the N-electron Schrödinger equation is the ultimate goal of electronic structure calculations, methods for obtaining these are neither sufficiently robust nor rigorously tested for general application, so that, *pro tempore* at least, one-electron solutions remain the most practicable, and most easily interpretable, alternative. Thus, solutions are sought to the one-electron equations

$$h\psi_i(i) = \varepsilon_i\psi_i(i)$$

where h is the one-electron Hamiltonian and the total N-electron wavefunction, $\Psi(1, \ldots, N)$, is given by

$$\Psi(1, \ldots, N) = \mathbf{a}\Pi_i\psi_i(i) \qquad \mathbf{a}\Pi_i\psi_i(i) \equiv \det|\psi_i(i)|.$$

Historically, two limiting one-electron approximations have been examined widely. They are the Hartree–Fock Hamiltonian, h_{HF},

$$\begin{aligned} h_{HF} &= T + V_N(\mathbf{R}) + J + X_e \\ &= h_0 + X_e \end{aligned}$$

where T, $V_N(\mathbf{R})$, J and X_e are the kinetic energy, external (nuclear) potential, electron–electron Coulomb and (exact) exchange operators, and the Kohn–Sham Hamiltonian, h_{KS}, which derives from density functional theory (DFT),

$$h_{KS} = h_0 + X_i(\rho) + C_i(\rho)$$

where X_i and C_i are the exchange and correlation contributions, which depend on the total electron density, ρ, and, at present, remain inexact. Both h_{HF} and h_{KS} have been used widely and successfully, but they have limitations in view of their approximate nature.

In an attempt to combine and exploit the virtues of both types of Hamiltonian, Becke [17] introduced a new class of so-called 'hybrid' Hamiltonians with the general form

$$h_{hyb}(\alpha, \beta) = h_0 + (1 - \alpha)X_e + \alpha X_i(\rho) + \beta C_i(\rho)$$

where α and β are arbitrary mixing parameters, such that for

$$\alpha, \beta = 0 \qquad h_{hyb} = h_{HF} \text{ (pure Hartree–Fock)}$$

and

$$\alpha, \beta = 1 \qquad h_{hyb} = h_{KS} \text{ (pure density functional)}$$

with $0 < \alpha, \beta < 1$ corresponding to the general hybrid Hamiltonian. In this paper we examine $h_{hyb}(\alpha, 1)$ for $0 \leqslant \alpha \leqslant 1$ and also $h_{hyb}(0, 0)$ ($\equiv h_{HF}$), based on the exchange and correlation functions within the generalized gradient approximation proposed by Perdew and Wang [18–20] and referred to hereafter as the PWGGA (hybrid) scheme. For convenience we refer to the two-parameter set $\{\alpha, 1\}$ by the single parameter F_0.

From a practical point of view, an appealing feature of hybrid Hamiltonians is that, in principle, values of α, β and F_0 might be derived by fitting to experimental data. This would render the approach essentially empirical, albeit based on first principles calculations, but there might still be some practical value to this approach if unique values for these constants could be found, even if they were system specific. However, recent studies have shown appreciable variation in hybridization parameters obtained by fitting to different properties of the same system [21, 22], so that an alternative use of the hybrid approach might be to examine and/or confirm the generic features and characteristics of systems across a broad range of hybridization. It is this latter use that we pursue here. Previous studies of NiO based on hybrid Hamiltonians have been reported by Bredow and Gerson [23], Moreira *et al* [24] and Muscat *et al* [25], who have examined the variation of properties such as the cohesive energy, band gap, and magnetic coupling constants with the proportion of exact exchange, but as far as we are aware there are no comparable studies of hole states.

2.3. Computational conditions

First principles, spin polarized, periodic Hartree–Fock and density functional theory based on localized atomic orbitals have been embodied within the CRYSTAL98 code [26]. In this study the crystal orbitals were expanded in a set of 25 orbitals for Ni of the type 1s(8), 2sp(6), 3sp(4), 4sp(1), 5sp(1), 3d(4), 4d(1), and 14 for O of the type 1s(8), 2sp(6), 3sp(4), 4sp(1), where the numbers 1, 2, 3, ... identify the different shells and the numbers in brackets are the numbers of primitive Gaussian type functions in the contraction for the atomic orbital. Open shell systems were treated by the spin-unrestricted (UHF) procedure [27]. The number and angular symmetry of the Gaussian functions used here are broadly similar to those employed recently by Moreira *et al* [24] in their hybrid DFT study of NiO. The implementation of DFT in the CRYSTAL98 code requires the specification of an auxiliary basis of Gaussian type functions for the fitting of the exchange–correlation potential. In this study we used simple bases consisting of 14 s-functions with exponents in the range 0.1–6000.0, and one d- and one g-function, each with an exponent 0.5, and 3 f-functions with exponents in the range 0.5–6.0 for Ni and 14 s-functions with exponents in the range 0.07–4000.0, and one p-, one d- and one f-function, each with an exponent of 0.5 for O. A Monkhorst–Pack shrinking factor of 8 and truncation thresholds of 10^{-7}, 10^{-7}, 10^{-7}, 10^{-7} and 10^{-14} for the Coulomb and exchange series [9] ensured convergence of the total UHF energies to $\leqslant$0.1 meV per molecule, while SCF convergence thresholds were set to 10^{-6} au for both eigenvalues and total energies.

As on previous occasions [13, 14], we have adopted a supercell approach to the electronic structure associated with the point defects Li'_{Ni}, $h^{\bullet}$ and $(Li'_{Ni}–h^{\bullet})^{x}$, wherein multiple unit cells containing individual defects at concentrations of 1/2, 1/4 and 1/8 are used to construct the periodic lattice. Defect concentrations of 1/4 and 1/8 are well within the range of the O k-edge and other spectroscopic data [5–8], while quadratic regressions based on these three concentrations allows rough estimates of the infinite dilution limit to be made. 2-, 4- and 8-fold unit cells with the ferromagnetic (FM) spin alignment and 8-fold cells with the antiferromagnetic (AF_2) alignment have been considered. Strictly speaking, the magnetic energy should be referenced to the paramagnetic state, but for convenience here we define the magnetic energy of an n-fold cell as $n^{-1}[E(AF_2) - E(FM)]$ and apply this definition both to the (non-defective) host lattice and to ionized states. Calculations have been carried out both at the full symmetry of the n-fold unit cell and in broken symmetry [13, 14]. The latter does not involve any change in the physical structure of the lattice, but is simply a formal reduction in symmetry, which allows, though does not force, a localization of the charge and net spin, if this leads to a lowering of the total energy. We define the hole localization energy simply

Table 1. Comparison of ground state properties of AF_2 and FM NiO as a function of F_0.

	E_{mag}	e_F (eV)		q_M (e)		n_s (μ_B)		$n^O_{e_F}$ (%)		E_g (eV)	
F_0	(meV/Ni)	AF_2	FM	AF_2	FM	AF_2	FM	AF_2	FM	AF_2	FM
UHF	19.7	−7.9	−7.7	1.87	1.87	1.92	1.93	92	86	14.8	14.2
1.0	22.2	−9.5	−9.3	1.88	1.88	1.92	1.92	92	87	14.2	14.0
0.9	25.3	−8.8	−8.6	1.87	1.87	1.91	1.92	92	85	13.1	12.7
0.8	29.2	−8.2	−7.9	1.86	1.86	1.90	1.92	89	85	12.1	11.5
0.7	34.0	−7.5	−7.2	1.84	1.85	1.88	1.89	87	82	10.9	10.3
0.6	40.1	−6.9	−6.5	1.82	1.83	1.86	1.88	83	80	9.8	9.0
0.5	50.6	−6.3	−5.8	1.80	1.81	1.84	1.86	76	77	8.7	8.0
0.4	69.2	−5.6	−5.2	1.77	1.78	1.80	1.83	71	74	7.4	6.8
0.3	90.0	−5.0	−4.5	1.73	1.75	1.76	1.79	71	70	6.4	5.5
0.2	117.1	−4.4	−3.8	1.68	1.71	1.69	1.75	41	64	4.5	4.4
0.1	169.2	−3.6	−3.0	1.62	1.65	1.59	1.69	11	57	2.6	3.2
0.0	277.7	−2.5	—	1.54	1.59	1.36	1.61	9	44	0.8	—

as the difference in energy between the localized and delocalized states. For the charged defects, Li'_{Ni} and $h^{\bullet}$, the lattice is embedded in a uniform charge compensating background to remove the Coulomb singularity [13, 14]. Mulliken population analyses [28] of the crystalline orbitals were used to extract the net atomic charges, magnetic moments and individual orbital occupations as in previous studies.

3. Results

3.1. Non-defective NiO

We begin by considering briefly the electronic structure of non-defective NiO (the host lattice) based on the PWGGA scheme at a fixed lattice constant of 4.2 Å, which is close to the measured low-temperature value, 4.1684 [9]. For this fixed structure, NiO is predicted to be a largely ionic, d^8 charge-transfer insulator from the correlated UHF limit (exact exchange) down to 30% exact exchange, with the antiferromagnetic AF_2 spin alignment lowest in energy. Within this range the Fermi energy, e_F, varies from −9.52 to −5.02 eV, the local spin moment from 1.92 to 1.76 μ_B, the filled-to-unfilled energy gap from 14.2 to 6.4 eV, and the weight of O(p) states at e_F from 92% to 71%. Between 30% and 20% exact exchange there is a change in the nature of the gap states, for at 20% exact exchange the weight of O(p) states at e_F is 41%, indicating an essentially Mott–Hubbard system, although the change in the ionic charge is <0.5% and that of the local moment <4%. As the amount of exact exchange is reduced further, the ionicity and local moment are decreased, though the system remains insulating at the DFT limit (0% exact exchange) where the weight of O(p) states at e_F is <10%, the local moment 1.36 μ_B, and the energy gap 0.8 eV.

From 100% exact exchange down to 30% there is essentially no difference in the electronic structures of the ferromagnetic (FM) and AF_2 spin alignments. Below this, the overall charge and spin distributions and Fermi level remain close, but there is no transition to a Mott–Hubbard system between 30% and 20% exact exchange for the FM alignment, as there is for AF_2. The other noteworthy difference between the two alignments is that for FM there is a displacement of the majority and minority spin bands of 0.5–1.0 eV, which at the DFT limit leads to a filled-to-unfilled gap of ∼0.3 eV for both the majority and minority spin bands, but a *net* gap which is close to zero. Overall, table 1 shows the close similarity between the FM and AF_2 electronic structures of NiO (except at the DFT limit) which is the basis for our more

Table 2. Comparison of some intrinsic ground state properties of pure and Li-doped FM NiO ($LiNi_7O_8^-$) as a function of the hybridization parameter, F_0.

	e_F (eV)		q_M (e)		n_s (μ_B)		$n^O_{e_F}$ (%)		E_g (eV)	
F_0	Li	Pure	Li	Pure	Li	Pure	Li	Pure	Li	Pure
UHF	−7.9	−7.7	1.86	1.87	1.92	1.93	86	86	14.2	14.2
1.0	−9.5	−9.3	1.86	1.88	1.92	1.92	85	87	13.9	14.0
0.9	−8.9	−8.6	1.85	1.87	1.91	1.92	85	85	12.7	12.7
0.8	−8.2	−7.9	1.84	1.86	1.90	1.92	83	85	11.5	11.5
0.7	−7.5	−7.2	1.83	1.85	1.88	1.89	83	82	10.3	10.3
0.6	−6.8	−6.5	1.81	1.83	1.87	1.88	80	80	9.2	9.0
0.5	−6.1	−5.8	1.79	1.81	1.84	1.86	78	77	8.0	8.0
0.4	−5.5	−5.6	1.76	1.78	1.81	1.83	75	74	6.9	6.8
0.3	−4.8	−5.0	1.73	1.75	1.78	1.79	70	70	5.7	5.5
0.2	−4.1	−4.4	1.69	1.71	1.73	1.75	65	64	4.5	4.4
0.1	−2.9	−3.0	1.64	1.65	1.66	1.68	55	57	3.2	3.2
0.0	−2.7	—	1.53	1.59	1.00	1.61	34	44	0.4	—

extensive use of the computationally more convenient (and less expensive) FM alignment in our study of defect states. In the context of the hybrid scheme, it might be of interest to note that the calculated moments for the AF_2 alignment compare with experimental values of 1.90 to 1.64 μ_B [9], which supports higher weights of exact exchange, whereas the measured strong adsorption edge, ∼4 eV [2], if it can be equated with the energy gap, E_g, would seem to favour a much lower weight. However, the close agreement of E_g in the region of 10%–20% exact exchange with the adsorption edge is problematic, for in this region the gap is predicted to be of Mott–Hubbard rather than charge-transfer character. These two examples confirm our earlier remarks concerning the variation in fitted hybridization parameters. The magnetic energy, as defined above, is one quantity that does vary quite considerably as a function of the proportion of exact exchange, ranging from 19.7 meV/Ni at the UHF limit to 277.7 meV/Ni for zero exact exchange. This evolution of the electronic structure as a function of exact exchange within the PWGGA scheme is similar to that reported by Bredow and Gerson [23] who based their calculations on Becke's B3LYP hybrid scheme [17].

Broadly speaking then, what might reasonably be deduced from the ground state electronic structure as to the nature of the first ionized, or hole state? Clearly the majority weight of oxygen states at the Fermi level from the UHF limit (∼90%) down to 30% exact exchange (∼70%) suggests holes of largely $d^8\underline{L}$ character. Mulliken charges and local moments suggest strong localization in the limit of exact exchange, with decreasing localization as the proportion of exact exchange is reduced. The increase in stability of the AF_2 state with decreasing exact exchange also suggests strong retention of the spin alignment for lower values of the hybridization parameter.

3.2. The electronic structure of Li'_{Ni}

Our calculations of the electronic structure of the uncompensated impurity defect, Li'_{Ni}, were based on FM 8-fold unit cells containing a single Li^+ substituent at a cation site, which, for convenience, we refer to as $LiNi_7O_8^-$. The principal objective here was to examine the extent to which the electronic structure of the host lattice is perturbed by the presence of an uncompensated Li^+ impurity. As in the case of the non-defective host lattice, the electronic structure of $LiNi_7O_8^-$ is obtained by direct variational minimization of the total energy of the 8-fold cell to self consistency. Table 2 compares the values of the Fermi energy, e_F, Mulliken

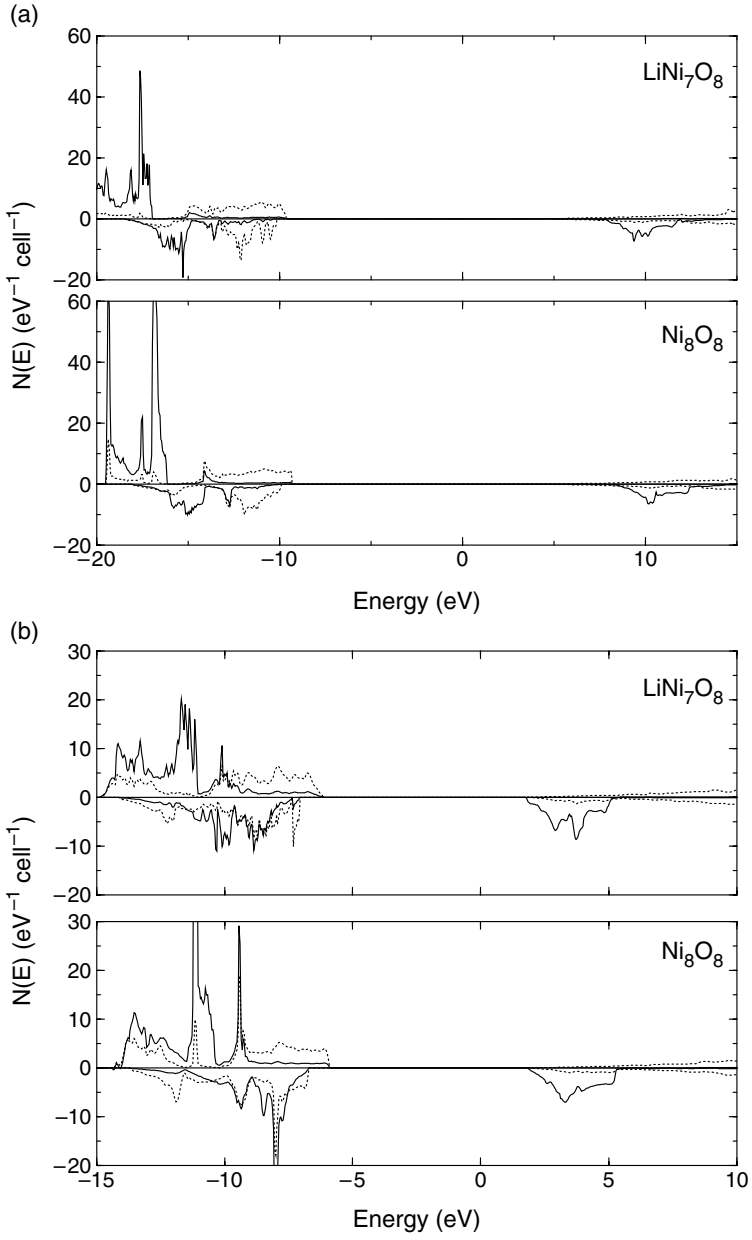

Figure 1. The valence and lower conduction band densities of states for the FM $LiNi_7O_8^-$ and FM Ni_8O_8 structures in the (a) 100% and (b) 50% hybrid schemes. (Full lines Ni states, dotted lines O states.)

charge of the nn oxygen ions, q_M, local spin moments at the nnn cation sites, n_s, weight of oxygen states at the Fermi level, $n^O_{e_F}$, and the filled-to-unfilled energy gap, E_g, for $LiNi_7O_8^-$ with those for the host lattice. Likewise, figure 1 compares the valence and lower conduction band densities of states for both 100% and 50% exact exchange. From these it is clear that, other than in the region of the DFT limit, the differences in the charge and spin distributions

and single-particle energies are marginal. Furthermore, the effective charge of Li'_{Ni} remains close to $-e$ for the full range of hybridization we have examined. This suggests that Li'_{Ni} behaves like an electronically inert entity with only a minor effect on the electronic, magnetic and excitonic properties of the host NiO lattice. It is reasonable to conclude, therefore, that the differences in the spectroscopic features of NiO and $Li_xNi_{1-x}O$ highlighted by Kuiper *et al* [5] and later studies [6–8] do not relate to Li'_{Ni} but to the presence of free and bound holes.

3.3. The free hole in NiO

We turn now to the free hole, the properties of which we deduce from the self-consistent electronic structures of 2-, 4- and 8-fold unit cells from which a single electron has been removed. The corresponding hole densities, or concentrations, are thus 0.5/NiO, 0.25/NiO and 0.125/NiO respectively, and, once again, the electronic structures of these periodically-arrayed, singly-charged unit cells are determined by direct variational minimization of the total cell energy. We recall that the lattice is immersed in a uniform charge-neutralizing background, which removes the Coulomb singularity, but has no effect on either the electronic charge ($\uparrow + \downarrow$) and spin ($\uparrow - \downarrow$) distributions or the differences in total energy between different states of the system. Our primary interests are the distribution of the hole charge between the cation and anion sublattices, the extent to which it is localized at one or more atomic sites, the different magnetic states of the hole and, importantly, whether the hole, or first ionized, state is insulating or conducting. For convenience, we define the hole charge and spin moment at a particular site as the differences between the Mulliken values for the non-defective host lattice and the singly-charged lattices.

We begin with the singly-ionized state of the FM lattice, for which there are four possible states corresponding to delocalized (d) and localized (l) charge and spin density with the unpaired electron spin either ferromagnetic, $(\Uparrow\uparrow)_d$ and $(\Uparrow\uparrow)_l$, or antiferromagnetic, $(\Uparrow\downarrow)_d$ and $(\Uparrow\downarrow)_l$, to the lattice spin. At the limit of 100% exact exchange, both with ($F_0 = 1.0$) and without (UHF) correlation, direct calculations for the three unit cells we have considered indicate that, as reported previously [14], in excess of 90% of the hole charge and spin are located on the anion sublattice, in accord with the charge-transfer character of the neutral ground state. For all three hole densities the $(\Uparrow\downarrow)$ spin configuration is of lower energy than $(\Uparrow\uparrow)$. Calculations in broken symmetry lead to insulating states with substantial localization of the hole charge on a single oxygen site, whereas calculations in full symmetry lead to conducting states of higher energy, in which the hole charge is delocalized over the anion lattice. Thus in the limit of exact exchange the first ionized state of NiO is predicted to be essentially $d^8\underline{L}$ with a non-zero energy gap and the majority of the hole charge and spin localized at a single oxygen site. The four states, $(\Uparrow\uparrow)_d$, $(\Uparrow\uparrow)_l$, $(\Uparrow\downarrow)_d$ and $(\Uparrow\downarrow)_l$, are in the order

$$E[(\Uparrow\downarrow)_l] < E[(\Uparrow\uparrow)_l] < E[(\Uparrow\downarrow)_d] < E[(\Uparrow\uparrow)_d].$$

Decreasing the proportion of exact exchange leads to a gradual and systematic change in the electronic structure of the first ionized state in two important respects. First, the stability of the localized state, $(\Uparrow\downarrow)_l$, increases relative to $(\Uparrow\uparrow)_l$, where the difference in energy between the two is the lowest lying excitation of the hole. This indicates that the spin pairing energy of the unpaired electron antiferromagnetic to the lattice in $(\Uparrow\downarrow)_l$ increasingly outweighs the direct exchange interaction of the unpaired electron ferromagnetic to the lattice in $(\Uparrow\uparrow)_l$. Second, there is a reduction of the localized hole charge and spin and a decrease in the localization energy down to approximately 40% exact exchange when there is a transition of both $(\Uparrow\downarrow)_l$ and $(\Uparrow\uparrow)_l$ to conducting states. At this phase transition the differences in energy between $(\Uparrow\downarrow)_l$

Table 3. (a) Energies (eV) of 8-unit FM $(\Uparrow\uparrow)_L$, $(\Uparrow\downarrow)_D$ and $(\Uparrow\uparrow)_D$ cells relative to $(\Uparrow\downarrow)_L$ as a function of F_0. (b) Comparison of localized hole charges, $q_h(e)$, and spin moments, n_s (μ_B), of 2-, 4-, 8- and ∞-unit FM $(\Uparrow\downarrow)_L$ cells as a function of F_0. (c) Comparison of localized hole charges, q_h (e), and unpaired oxygen spin moments, n_s (μ_B), of 8-unit FM $(\Uparrow\downarrow)_L$ and $(\Uparrow\uparrow)_L$ alignments as a function of F_0.

(a)	F_0	$(\Uparrow\uparrow)_L$	$(\Uparrow\downarrow)_D$	$(\Uparrow\uparrow)_D$
	UHF	0.47	2.28	3.70
	1.0	0.51	2.17	3.59
	0.9	0.56	1.74	3.08
	0.8	0.61	1.33	2.59
	0.7	0.67	0.94	2.13
	0.6	0.72	0.59	0.83
	0.5	0.78	0.25	0.26
	0.4	0.09	0.04	—

		2FM		4FM		8FM		∞FM	
(b)	F_0	q_h	n_s	q_h	n_s	q_h	n_s	q_h	n_s
	UHF	0.85	0.88	0.81	0.87	0.77	0.85	0.71	0.82
	1.0	0.84	0.87	0.80	0.86	0.76	0.84	0.70	0.80
	0.9	0.82	0.85	0.78	0.84	0.73	0.81	0.65	0.76
	0.8	0.80	0.82	0.75	0.81	0.68	0.77	0.59	0.70
	0.7	0.76	0.78	0.71	0.77	0.63	0.71	0.51	0.61
	0.6	0.72	0.73	0.65	0.71	0.55	0.62	0.40	0.48
	0.5	0.66	0.67	0.58	0.62	0.45	0.49	0.27	0.30
	0.4	0.47	0.39	0.20[a]	0.09[a]	0.11[a]	0.04[a]	0.05	0.06

		q_h		n_s	
(c)	F_0	$(\Uparrow\downarrow)_L$	$(\Uparrow\uparrow)_L$	$(\Uparrow\downarrow)_L$	$(\Uparrow\uparrow)_L$
	UHF	0.77	0.80	0.85	0.98
	1.0	0.76	0.79	0.84	0.97
	0.9	0.73	0.76	0.81	0.96
	0.8	0.68	0.73	0.77	0.94
	0.7	0.63	0.67	0.71	0.90
	0.6	0.55	0.59	0.62	0.83
	0.5	0.45	0.47	0.49	0.71
	0.4	0.11[a]	0.09	0.04[a]	0.07

[a] Conducting state.

and $(\Uparrow\uparrow)_l$ and $(\Uparrow\downarrow)_d$ and $(\Uparrow\uparrow)_d$ all fall to <0.1 eV and the asymmetries in the charge and spin distributions associated with $(\Uparrow\downarrow)_l$ and $(\Uparrow\uparrow)_l$ disappear. Since there is no evidence that $Li_xNi_{1-x}O$ is conducting in the range, $0 \leqslant x \leqslant 0.5$, we have not considered FM alignments with less than 40% exact exchange in this study. Full details of the energies of the $(\Uparrow\uparrow)_l$, $(\Uparrow\downarrow)_d$ and $(\Uparrow\uparrow)_d$ states of 8-unit FM cells relative to $(\Uparrow\downarrow)_l$ as a function of F_0 are contained in table 3(a), while table 3(b) contains the local charge and spin of 2-, 4-, 8- and ∞-unit FM $(\Uparrow\downarrow)_l$ cells, again as a function of F_0. The values for the ∞-unit cells, i.e. the isolated free hole, were obtained from quadratic regressions of the 2-, 4-, 8-unit charges and spin moments as a function of n^{-1}.

To investigate the influence of the antiferromagnetic spin alignment of the host lattice, we have carried out similar direct calculations for 8-unit AF_2 cells, for which there is only one alignment of the unpaired spin. Once again, calculations in full and broken symmetry yield delocalized and localized hole states, respectively. Table 4 compares local hole charges,

Table 4. Comparison of 8-unit AF_2 and ($\Uparrow\downarrow$) local hole charges, $q_h(e)$, spin moments, n_s (μ_B) and localization energies, E_{loc} (eV) and ΔE_{loc} (eV), and the magnetic energies, E_{mag} (meV), of the host lattice and localized AF_2 hole.

	q_h		n_s		E_{mag}		E_{loc}		
F_0	AF_2	FM	AF_2	FM	Host	h_L	AF_2	FM	ΔE_{loc}
UHF	0.78	0.77	0.91	0.85	19.7	−92.9	2.32	2.28	0.04
1.0	0.78	0.76	0.90	0.84	22.2	−106.7	2.20	2.17	0.03
0.9	0.76	0.72	0.88	0.81	25.3	−107.7	1.81	1.74	0.07
0.8	0.72	0.68	0.86	0.77	29.2	−109.7	1.43	1.33	0.10
0.7	0.67	0.63	0.81	0.71	34.0	−109.7	1.05	0.94	0.11
0.6	0.60	0.55	0.74	0.62	40.1	−95.1	0.68	0.59	0.09
0.5	0.50	0.45	0.63	0.49	50.6	−104.3	0.41	0.25	0.16
0.4	0.36	0.11[a]	0.48	0.04[a]	69.2	−75.0	0.23	0.04[a]	0.19

[a] Conducting state.

spin moments, magnetic and localization energies of AF_2 and ($\Uparrow\downarrow$) FM spin alignments as a function of the proportion of exact exchange. Also included is the variation of the magnetic energy of the host lattice. From this it is clear that while the AF_2 alignment stabilizes the localized state to the extent that it remains insulating down to 20% exact exchange with a filled-to-unfilled gap of ∼0.7 eV at 40%, the hole charge and spin distributions are largely independent of the alignment of the lattice moments, as are the atomic charges and cation moments of the non-defective lattice. The delocalization energy is also largely independent of the spin alignment, as might have been predicted, since it is approximately three orders of magnitude larger than the magnetic energy of the non-defective host lattice. However, what table 4 shows quite clearly is that the ($\Uparrow\downarrow$) FM spin alignment is more stable than the AF_2 alignment by ∼100 meV from the UHF limit down to 50% exact exchange. In other words, flipping three of the Ni spins nn to the unpaired electron leads to a substantial lowering of the energy. Again, this might have been expected from the relative stability of the FM $(\Uparrow\downarrow)_1$ and $(\Uparrow\uparrow)_1$ states, for half their differences in energy, given in table 3(a), is appreciably greater than the magnetic energy of the host lattice. Thus our calculations predict that the first ionized state in AF_2 NiO is essentially $d^8\underline{L}$ with strong spatial and spin polaron character. Furthermore, the magnitudes of the delocalization and magnetic energies given in table 4 suggest that both the spatial and spin polaronic character will persist into the paramagnetic phase.

3.4. The Li-bound hole in NiO

Our study of the bound hole involves the single system, $Li_{0.125}Ni_{0.875}O$, which we model by the 8-unit cell $LiNi_7O_8$, and which is confined to the FM spin alignment. We recall that our primary interests are in the differences between the electronic structures of the free and bound hole, here $Ni_8O_8^+$ and $LiNi_7O_8$, and the way the electronic structure varies with the hybridization, or proportion of exact exchange, of the one-electron Hamiltonian. Once again calculations have been performed in full and broken symmetry and in both spin alignments of the unpaired spin. They range from the UHF limit down to 40% exact exchange, in the vicinity of which there is a transition of the free hole state, $Ni_8O_8^+$, from insulating to conducting. Starting at the limit of exact exchange, direct minimization of the total energy leads to states in which over 90% of the hole charge resides on the oxygen sublattice and in exactly the order found for the free hole. In other words, we find essentially the same $d^8\underline{L}$ electronic configuration for the free and bound hole. Table 5(a) compares the local hole charges and spin

Table 5. (a) Comparison of localized hole charge, q_h (e), spin moment, n_s (μ_B) and energy (eV) differences, $\Delta E_{\Uparrow\downarrow-\Uparrow\uparrow}(L)$ and $\Delta E_{LD}(\Uparrow\downarrow)$ for $Ni_8O_8^+$ (8FM) and $LiNi_7O_8$ (Li7FM) and the Li–hole binding energy, E_{bind} (eV) in $LiNi_7O_8$. (b) Comparison of the edge-to-edge $d^8\underline{L}$–d^9 gap (eV) for 8FM$(\Uparrow\downarrow)_L$, Li7FM $(\Uparrow\downarrow)_L$ and $8AF_2$ as a function of F_0.

		q_h		n_s		$\Delta E_{\Uparrow\downarrow-\Uparrow\uparrow}(L)$		$\Delta E_{LD}(\Uparrow\downarrow)$		
(a)	F_0	8FM	Li7FM	8FM	Li7FM	8FM	Li7FM	8FM	Li7FM	E_{bind}
	UHF	0.77	0.81	0.85	0.90	0.47	0.15	2.28	3.10	0.59
	1.0	0.76	0.81	0.84	0.89	0.51	0.19	2.17	2.97	0.57
	0.9	0.73	0.79	0.81	0.89	0.56	0.21	1.74	2.43	0.60
	0.8	0.68	0.75	0.77	0.84	0.61	0.23	1.33	1.88	0.64
	0.7	0.63	0.70	0.71	0.79	0.67	0.27	0.94	1.36	0.67
	0.6	0.55	0.63	0.62	0.70	0.72	0.31	0.59	0.85	0.71
	0.5	0.45	0.46	0.49	0.52	0.78	0.35	0.25	0.41	0.81
	0.4	0.11[a]	0.26	0.04[a]	0.17	0.09[a]	0.49	0.04[a]	0.11	0.81

(b)	F_0	8FM	$8AF_2$	Li7FM
	UHF	4.0	4.4	4.0
	1.0	3.8	4.1	3.5
	0.9	4.0	4.4	4.0
	0.8	4.3	4.8	4.2
	0.7	4.5	5.1	4.5
	0.6	4.7	5.3	4.8
	0.5	4.7	5.6	5.1
	0.4	5.4[a]	4.6	4.8

[a] Conducting states.

moments, the differences in energy between the two spin alignments of the localized hole, $\Delta E_{\Uparrow\downarrow-\Uparrow\uparrow}(L) = E[(\Uparrow\downarrow)_l] - E[(\Uparrow\uparrow)_l]$, and the localization energies for the antiferromagnetic alignment, $\Delta E_{LD}(\Uparrow\downarrow) = E[(\Uparrow\downarrow)_l] - E[(\Uparrow\downarrow)_d]$, of $LiNi_7O_8$ and $Ni_8O_8^+$. Also given is the unrelaxed binding energy of Li'_{Ni} and the localized hole, E_{bind}, in $LiNi_7O_8$. From this two general points emerge. The first is that the evolution of the electronic structure of the bound hole as the proportion of exact exchange is reduced follows a similar pattern to that of the free hole; the second is that, as expected, the presence of the charge compensating defect, Li'_{Ni}, with an effective charge close to $-e$, stabilizes the localized hole. Thus we find the local charge and spin moment of the bound hole to be ∼5% greater than the free hole, and the localization energy ∼30% greater across the range of exact exchange we have considered. Our estimates of E_{bind}, which we obtain directly from the energies of $LiNi_7O_8$, $LiNi_7O_8^-$, $Ni_8O_8^+$ and the host lattice, range from 0.59 eV at the UHF limit to 0.81 eV at 40% exact exchange. A further indication of the stabilizing effect of Li'_{Ni} is that for 40% exact exchange, the free hole state is predicted to be conducting, whereas there is a filled-to-unfilled gap of ∼0.4 eV for the bound hole. For all values of F_0 we have considered, the (local) charge, spin moment and localization energy of the bound hole, $\Delta E_{LD}(\Uparrow\downarrow)$, are greater than those for the free hole. Correspondingly, the spin alignment energy, $\Delta E_{\Uparrow\downarrow-\Uparrow\uparrow}(L)$, is less.

In both the original report of the oxygen k-edge absorption of $Li_xNi_{1-x}O$ by Kuiper *et al* [5] and subsequent studies [6–8], one of the most noteworthy features of the spectra is the gap of ∼4 eV between absorptions attributed to the $O(1s)^2 + d^8\underline{L} \rightarrow O(1s)^1 + d^8$ and $O(1s)^2 + d^8\underline{L} \rightarrow O(1s)^1 + d^9\underline{L}$ transitions, in which an O(1s) electron is excited into an O(2p) hole in the former and into the p states of the conduction band in the latter. This is close to the energy of the strong absorption edge of NiO [2] which is often identified with the calculated

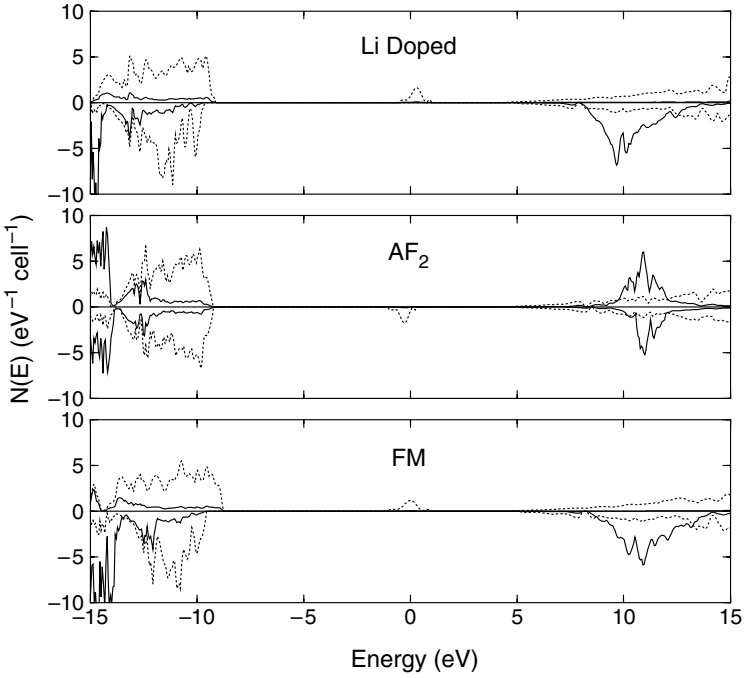

Figure 2. The valence, hole and conduction band densities of states for the bound hole in FM(⇑↓) $LiNi_7O_8$ and the free hole in FM (⇑↓) and AF_2 Ni_8O_8. (Full lines Ni states, dotted lines O states.)

charge transfer gap. It is both well known, and also clear from table 1, that for high proportions of exact exchange, notably at the UHF limit, the calculated energy gap is much greater than the adsorption edge, a reasonable explanation for which is the strong renormalization of the valence states that accompanies the charge transfer excitation from the valence to the conduction band. While similar renormalizations are likely to occur for the transitions involved in the oxygen k-edge spectra, if the renormalization energies are similar, the gap between the calculated empty O(2p) state associated with the hole and the conduction band edge would be expected to be close to 4 eV. Table 5(b) contains the calculated gap between the empty O(2p) band and the conduction band lower edge, or $d^8\underline{L}$–d^9 gap, as it is sometimes referred to [5], for $Ni_8O_8^+$ and $LiNi_7O_8$ as a function of the proportion of exact exchange. As is seen in figure 2, which corresponds to 100% exact exchange, the gaps associated with the free and bound holes within the insulating regime are barely distinguishable, in accord with the observation of a single absorption peak, and for high proportions of exact exchange close to 4 eV.

4. Discussion

As is often the case in the defect physics of solids, elucidating the differences in the electronic and magnetic properties of closely related point defects is a difficult experimental task, which calculations should, in principle, facilitate. In this study based on a hybrid UHF-DFT one-electron approach to the electronic structure, we have attempted to elucidate such differences for the hole-related defects in the paradigm system, $Li_xNi_{1-x}O$ which, at high temperature, at least, can be represented by three types of point defect, Li'_{Ni}, $h^\bullet$ and $(Li'_{Ni}$–$h^\bullet)^x$ in an NiO

host lattice. We have also examined the extent to which one-electron Hamiltonians containing varying proportions of exact exchange paint different pictures of the electronic structures of these defects. Starting with Li'_{Ni}, calculations within the full range of exact exchange from UHF to DFT suggest that it is inert electronically, with negligible perturbation of the electronic structure of the host lattice, despite its effective charge close to $-e$. It is reasonable to conclude, therefore, that other than as a potential site for hole capture, Li'_{Ni} plays no part in the electronic properties of $Li_xNi_{1-x}O$.

The nature of the compensating hole, both free carrier, $h^\bullet$, and bound charge, $(Li'_{Ni}–h^\bullet)^x$, follows from the charge transfer character of the host lattice and is essentially $d^8\underline{L}$ for the entire range of hybridization we have considered. For high proportions of exact exchange the charge and spin densities of the free hole are largely localized at a single oxygen site, with localization energies in excess of 2 eV for both the AF_2 and FM spin alignments and filled-to-unfilled gaps in excess of 5 eV. For the hypothetical, though computationally convenient FM spin configuration, the antiferromagnetic alignment of the unpaired oxygen spin with respect to the FM lattice moments, ($\Uparrow\downarrow$), is favoured over the ferromagnetic alignment, ($\Uparrow\uparrow$). Evidently, the energy of the partial (spin) pairing between the unpaired oxygen spin and the six antiferromagnetically aligned nn Ni spins in ($\Uparrow\downarrow$) is greater than the direct exchange energy between the unpaired oxygen spin and the six ferromagnetically aligned nn Ni spins in ($\Uparrow\uparrow$). That partial spin pairing occurs is seen clearly in table 3(c), which shows that while the localized hole charges in ($\Uparrow\downarrow$) and ($\Uparrow\uparrow$) differ by less than 5%, the unpaired oxygen spin moments in ($\Uparrow\downarrow$) are less than those in ($\Uparrow\uparrow$) by up to 40% as a result of the overlap with the neighbouring Ni spins. The differences in energy between these two spin configurations vary from ∼80 meV/Ni to ∼130 meV/Ni over the range of exact exchange we have considered, so that even in the absence of explicit calculations for the AF_2 hole state, the FM ($\Uparrow\downarrow$) alignment would be expected to be lower in energy. Direct comparisons of the total energies given in table 4(a) confirm this to be the case, leading to the prediction of spin polaron behaviour in which a localized unpaired oxygen spin in AF_2 NiO is surrounded by six antiferromagnetically aligned Ni spins which accompany its activated migration. As the proportion of exact exchange is reduced, the charge and spin densities in both the FM and AF_2 alignments delocalize, with corresponding decreases in both the localization energy and filled-to-unfilled gap. In the case of both FM alignments this leads to metallic states between 50% and 40% exact exchange, whereas the AF_2 alignment remains insulating down to 20%, even though it remains higher in energy than FM ($\Uparrow\downarrow$). The electronic structure of the bound hole, $(Li'_{Ni}–h^\bullet)^x$, is found to be very similar to that of the free hole, allowing for the stabilizing effect of Li'_{Ni} on $h^\bullet$. The $Li'_{Ni}–h^\bullet$ binding energy in an atomically unrelaxed lattice is in the region of 0.7 eV, and for a given proportion of exact exchange, localized hole charges and spin moments are slightly greater in $(Li'_{Ni}–h^\bullet)^x$ than $h^\bullet$, but crucially from a spectroscopic point of view, the $d^8\underline{L}$–d^9 gaps are very close, leading to the prediction of a single gap in $Li_xNi_{1-x}O$, in agreement with the reported oxygen k-edge and other spectra [5]. The stabilizing effect of Li'_{Ni} is also manifest in the preservation of a filled-to-unfilled gap at 40% exact exchange where the free hole state is metallic.

The objective of this study was to examine the influence of hybridization on the properties of hole states in NiO, and our principal conclusions in this regard are fourfold. The first is that over a wide range of exact exchange, notably where both the free and bound carrier are insulating, the hole state is essentially $d^8\underline{L}$, in agreement with spectroscopic studies [5–8], with substantial proportions of the hole charge and unpaired spin located at a single oxygen site. Second, that the electronic structure of the free hole is largely independent of the spin alignment of the lattice, but that partial spin pairing of the unpaired electron with nearest neighbour Ni spins which are antiferromagnetically aligned, leads to strong spin polarization

Table 6. Comparison of PWGGA and B3LYP values of the unpaired spin moment, n_s (μ_B), localization energy, E_{loc} (eV) and the edge-to-edge $d^8\underline{L}$–d^9 gap, E_g (eV) for and $8AF_2$ cells as a function of F_0.

	n_s		E_{loc}		E_g	
F_0	PWGGA	B3LYP	PWGGA	B3LYP	PWGGA	B3LYP
UHF	0.91	0.91	2.32	2.32	4.4	4.4
1.0	0.91	0.90	2.20	2.27	4.1	4.6
0.9	0.89	0.88	1.81	1.82	4.4	4.9
0.8	0.86	0.86	1.43	1.43	4.8	5.1
0.7	0.81	0.81	1.05	1.03	5.1	5.4
0.6	0.75	0.74	0.68	0.73	5.3	5.7
0.5	0.63	0.63	0.41	0.43	5.6	5.5
0.4	0.48	0.48	0.23	0.22	4.6	4.5
0.3	0.27	0.25	0.06	0.02	3.7	3.4
0.2	0.17	0.17	0.07	0.10	2.4	2.3

of the surrounding lattice. Third, that decreasing the proportion of exact exchange leads to a delocalization of the charge and spin and corresponding decrease in the localization energy, with a transition to a conducting state of the low-energy FM ($\Uparrow\downarrow$) alignment, and by implication the spin polaron, between 40% and 50%. Fourth, that the evolution of the electronic structure of the bound hole with F_0 follows a very similar pattern to that of the free carrier. Finally, to assess, albeit briefly, the extent to which the PWGGA scheme gives a representative view of the effects of hybridization, we have examined the free hole in the AF_2 spin alignment based on the B3LYP scheme [17]. Table 6 compares the unpaired spin moment at the hole site, n_s, the localization energy, E_{loc}, and the edge-to-edge $d^8\underline{L}$–d^9 gap, E_g, for AF_2 $Ni_8O_8^+$ as a function of F_0 for the two schemes. From this it is clear that while there are small differences between the two, notably in the $d^8\underline{L}$–d^9 gap, overall the evolution of the electronic structure of the free hole state is very similar, so that our study would seem to capture the generic effects of hybridization.

While the present view of holes states in NiO differs from that assumed by Norgett *et al* [15] in that the weight of evidence, both theoretical and experimental, suggests they are essentially $d^8\underline{L}$ rather than d^7, their predicted local character, in terms of both charge and spin, preserves an important link with ideas and methodology that Michael Norgett developed so successfully.

Acknowledgment

DSM wishes to thank the EPSRC for the award of a research studentship, during the tenure of which the work reported here was carried out.

References

[1] Hüfner S 1994 *Adv. Phys.* **43** 183
[2] Powell R J and Spicer W E 1970 *Phys. Rev.* B **2** 2182
[3] Terakura K, Oguchi T, Williams A R and Kübler J 1984 *Phys. Rev.* B **30** 4734
[4] Zaanen J, Sawatzky G A and Allen J W 1984 *Phys. Rev. Lett.* **55** 418
[5] Kuiper P, Kruizinga G, Ghijsen J and Sawakzky G A 1989 *Phys. Rev. Lett.* **62** 221
[6] Hüfner S, Steiner P, Sander I, Reinert F, Schmitt H, Neumann M and Witzel S 1991 *Solid State Commun.* **80** 869
[7] van Elp J, Searle B G, Sawatzky G A and Sacchi M 1991 *Solid State Commun.* **80** 67

[8] van Elp J, Eskes H, Kuiper P and Sawatzky G A 1992 *Phys. Rev.* B **45** 1612
[9] Towler M D, Allan N L, Harrison N M, Saunders V R, Mackrodt W C and Aprà E 1994 *Phys. Rev.* B **50** 5041
[10] Szotek Z, Temmerman W M and Winter H 1993 *Phys. Rev.* B **47** 4029
[11] Anisimiv V I, Zaanen J and Andersen O K 1991 *Phys. Rev.* B **44** 943
[12] Massidda S, Continenza A, Posternak M and Baldereschi A 1997 *Phys. Rev.* B **55** 13494
[13] Mackrodt W C, Harrison N M, Saunders V R, Allan N L and Towler M D 1996 *Chem. Phys. Lett.* **250** 66
[14] Mackrodt W C 1997 *Ber. Bunsenges. Phys. Chem.* **101** 169
[15] Catlow C R A, Mackrodt W C, Norgett M J and Stoneham A M 1977 *Phil. Mag.* **35** 177
Catlow C R A, Mackrodt W C, Norgett M J and Stoneham A M 1979 *Phil. Mag.* **40** 161
[16] Kröger F 1964 *The Chemistry of Imperfect Crystals* (Amsterdam: North-Holland)
[17] Becke A D 1993 *J. Chem. Phys.* **98** 5648
[18] Perdew J P and Wang Y 1986 *Phys. Rev.* B **33** 8800
[19] Perdew J P and Wang Y 1989 *Phys. Rev.* B **40** 3399
[20] Perdew J P and Wang Y 1992 *Phys. Rev.* B **45** 13244
[21] Corà F, Alfredsson M, Mallia G, Middlemiss D S, Mackrodt W C, Dovesi R and Orlando R 2004 *Structure and Bonding* (Berlin: Springer) at press
[22] Mackrodt W C, Middlemiss D S and Owens T G 2004 *Phys. Rev.* B at press
[23] Bredow T and Gerson A R 2000 *Phys. Rev.* B **61** 5194
[24] Moreira I de P R, Illas F and Martin R L 2002 *Phys. Rev.* B **65** 155102
[25] Muscat J, Wander A and Harrison N M 2001 *Chem. Phys. Lett.* **342** 397
[26] Saunders V R, Dovesi R, Roetti C, Causà M, Harrison N M, Orlando R and Zicovich-Wilson C M 1998 *CRYSTAL98, User's Manual* (Torino: University of Torino)
[27] Pople J A and Nesbet R K 1954 *J. Chem. Phys.* **22** 571
[28] Mulliken R S 1955 *J. Chem. Phys.* **23** 1833
Mulliken R S 1955 *J. Chem. Phys.* **23** 1841